

Proceedings Article

# Trade-off between power consumption and receive signal strength for inductively coupled transmit-receive circuits in MPI

Fabian Mohn <sup>a,b,\*</sup> · Fynn Foerger <sup>a,b</sup> · Florian Thieben <sup>a,b</sup> · Martin Möddel <sup>a,b</sup> · Tobias Knopp <sup>a,b,c</sup> · Matthias Graeser <sup>c,d</sup>

<sup>a</sup>Section for Biomedical Imaging, University Medical Center Hamburg-Eppendorf, Hamburg, Germany

<sup>b</sup>Institute for Biomedical Imaging, Hamburg University of Technology, Hamburg, Germany

<sup>c</sup>Fraunhofer IMTE, Fraunhofer Research Institution for Individualized and Cell-based Medical Engineering, Lübeck, Germany

<sup>d</sup>Institute of Medical Engineering, University of Lübeck, Lübeck, Germany

\*Corresponding author, email: [fabian.mohn@tuhh.de](mailto:fabian.mohn@tuhh.de)

© 2024 Mohn *et al.*; licensee Infinite Science Publishing GmbH

This is an Open Access article distributed under the terms of the Creative Commons Attribution License (<http://creativecommons.org/licenses/by/4.0>), which permits unrestricted use, distribution, and reproduction in any medium, provided the original work is properly cited.

## Abstract

The signal chain of a Magnetic Particle Imaging system can be designed to include a dedicated receive-only coil or to combine transmit and receive coils. More common are circuits with separate transmit and receive chains, using dedicated receive coil(s) that cancel the excitation feedthrough. However, combined transmit-receive systems may prove to have several benefits, such as reducing the system complexity, providing a lower resistive noise contribution due to larger copper cross-section, facilitating a transition from 1D to multidimensional signal generation and acquisition, and implementing an embedded band-stop filter. In this theoretical work, a matching condition that governs inductors for resonant combined transmit-receive systems is investigated. To tap the signal, a compromise between the obtained signal strength and power consumption is considered, caused by the chosen circuit topology, that balances both signal loss and power consumption at a  $-3$  dB benchmark.

## 1. Introduction

Magnetic Particle Imaging (MPI) signals typically need to be acquired simultaneously during signal generation due to the fast relaxation and weak induction of magnetic nanoparticles (MNPs) [1]. Thus, the extraction of the nonlinear receive signal is a crucial challenge of MPI, which is typically done by filtering the fundamental to exclude direct signal feedthrough from excitation and to preserve the important signal harmonics. Since the initial patent of MPI in 2001 by scientists at Philips Research in Hamburg, different approaches to signal generation and detection have been realized to optimize the quality of the receive signal [2, 3]. A significant difference lies in the general topology of the signal chain, which

can be broadly categorized into two classes: circuits using dedicated receive coils [4, 5] and combined transmit-receive circuits (TxRx) [6, 7]. The majority of MPI systems employs dedicated receive coils [3], which is a straight forward approach to obtain a clean receive signal [8, 9].

In this theoretical work, we briefly review the advantages of different approaches to the MPI signal chain and determine a specific matching condition for combined transmit-receive circuits that use an inductive coupling network (ICN), based on the work of Sattel *et al.* [6]. We go into the details of an ICN and how the (secondary) inductor should be chosen with regard to the inductance of the drive field generator (DFG). Finally, a trade-off is presented that considers the voltage level of the particle signal versus the power consumed at resonance.

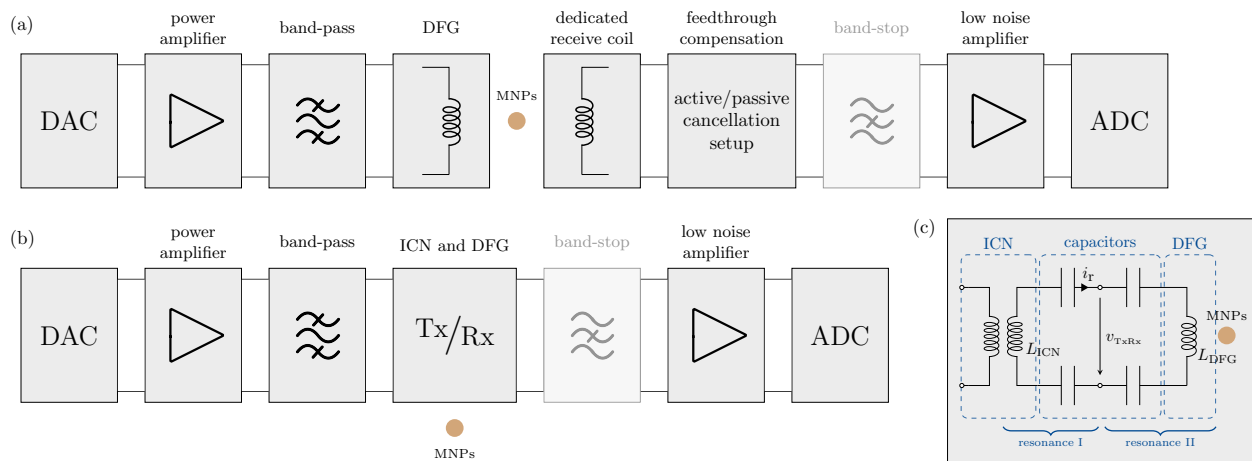


**Figure 1: Two MPI Signal chain topologies.** (a) Signal chain including a dedicated receive-only coil, that is coupled to the transmit coil (drive field generator (DFG)) and requires feedthrough compensation. (b) Transmit-receive circuit that uses the DFG for signal generation and acquisition. A band-stop filter is optional, because a filter of the fundamental  $f_1$  is embedded by the symmetric split of the capacitors, as shown in (c). Here, the circuit within the  $T_x/R_x$  box is shown, which is composed of the ICN, 4 capacitor banks and the DFG. The receive signal  $v_{TxRx}$  is tapped across the inductances  $L_{ICN}$  and  $L_{DFG}$  which become high impedances at higher harmonics and the capacitors become fully conductive.

## II. Motivation

An overview of two signal chain topologies is given in Figure 1 (a) and (b), for dedicated and for combined TxRx circuits, respectively. The focus of this work lies on the symmetric and resonant TxRx circuit, which is shown in detail in Figure 1 (c) that represents the  $T_x/R_x$  box of (b). The motivation is to determine the governing conditions that affect the choice of  $L_{ICN}$  for a given  $L_{DFG}$ . We assume a toroidal configuration with an air-core for maximum linearity, as the feed-in of the resonant circuit.

**Dedicated receive circuit.** An advantage of dedicated receive circuits is the gradiometer configuration [8]. By superimposing a  $180^\circ$  phase shifted signal, all coupled signal influences contained in the field are canceled if wire dimensions remain below a small fraction of the wavelength. This includes not only the coupled excitation fundamental, but also interference, systemic harmonics and systemic fluctuations [10]. Due to opposing voltage induction, circulating currents are low and thin litz-wire can be used with more windings than the transmit coil. This linearly increases the receive signal, which is beneficial as long as the coil noise is not dominant in the system. The gradiometer can be further combined with active suppression [11] or resonators [12] to improve the sensitivity [9, 13].

**Combined transmit-receive circuit.** The TxRx circuit uses the same coil (per spatial direction) for signal generation and acquisition. Thus, it saves valuable space and can be placed closer to the bore. Also, multi-channel systems only require a single coil(-pair) per channel, which facilitates measures against crosstalk (inductive coupling) within the DFG, because coupling to dedi-

cated coils and in-between cancellation windings does not need to be considered. Furthermore, signal generating coils typically have a large copper cross-section and lower resistance than receive-only coils (thin Litz wire, many turns), which reduces thermal noise, motivated by reaching patient-noise dominance [14]. TxRx systems can either tap the coil directly in combination with a band-stop filter [7] or a resonant symmetric schematic acts as a band-stop filter of the excitation frequency  $f_1$ : two nodes (virtual ground) are created by splitting the capacitor banks, which creates the signal tap  $v_{TxRx}$  [6]. Thus, virtual ground refers to the fact that no potential is measured at  $f_1$  across  $v_{TxRx}$  within the resonator. Here, the signal  $v_{TxRx}$  is influenced by the inductors  $L_{ICN}$  and  $L_{DFG}$ , more precisely by their ratio, forming a central condition that is investigated in the following.

## III. Methods and materials

We assume a fixed coil  $L_{DFG}$ , given by geometric and topological decisions, and consider the resonant TxRx circuit of Figure 1 (c) with a fixed current  $i_t$  for a specific excitation field. We define the total series resistance  $R_s$  as the sum of all resistances within the resonator of Figure 1 (c), namely the equivalent series resistance of ICN  $R_{ICN}$  and DFG  $R_{DFG}$ , as well as connections. The resistance of capacitors, connection losses and the DFG are constant. Further, the quality factor  $Q_{ICN} = 2\pi f_1 L_{ICN}/R_{ICN}$  is constant, because it is assumed to be restricted by an available finite construction volume for a chosen wire. This results in a linear relationship of the series resistance  $R_{ICN} \sim R_s$  and  $L_{ICN}$ .

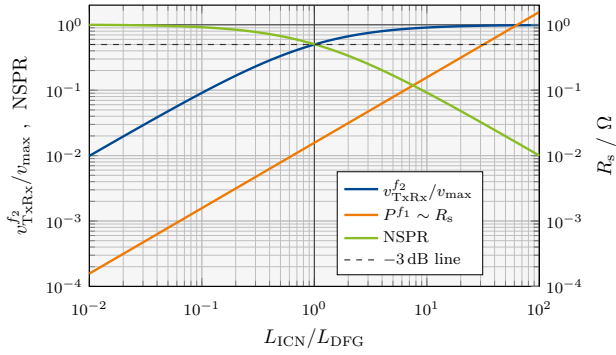


**Figure 2: Inductance matching condition.** The choice of  $L_{ICN}$  is restricted by the trade-off between particle signal level (blue) and power consumption (orange). The normalized signal to loss ratio (NSPR, green) expresses the additionally required power to obtain a stronger receive signal. For the case of  $L_{ICN} = L_{DFG}$ , the receive signal is halved ( $-3$  dB).

Two conflicting objectives restrict the choice of  $L_{ICN}$ : Achieving maximum particle signal strength and minimum power consumption. The particle signal is maximal if  $L_{ICN} \gg L_{DFG}$ , due to the inductive voltage divider formed by these two inductors at high frequencies. If  $L_{DFG}$  is conceptualized as a distributed voltage source, inducing the particle voltage at the nodes of  $v_{TxRx}$ , a small  $L_{ICN}$  would short circuit the receive signal. As the quality factor is considered constant, an increase of  $L_{ICN}$  necessarily causes the same increase in series resistance  $R_{ICN}$  of the toroid and therefore increases the total power consumption via  $R_s$ . Thus, a partial attenuation of the particle signal is inevitable for feasible  $L_{ICN}$ , imposed by field specifications for  $i_r$  and the finite available power. To express this trade-off, we consider a unit current  $i_r = 1$  A at  $f_1$ , and define the particle signal-to-power ratio (SPR)

$$SPR = \frac{v_{TxRx}^{f_2}}{P^{f_1}} = \frac{v_{TxRx}^{f_2}}{i_r^2 R_s}. \quad (1)$$

The crucial point is that the particle signal  $v_{TxRx}^{f_2}$  is considered at a higher frequency  $f_2$ , but the power  $P^{f_1}$  is considered at resonance  $f_1$ . The SPR is a function of  $L_{ICN}$  via its relation to  $R_s$ .  $v_{max}$  describes the maximum voltage of  $v_{TxRx}^{f_2}$  in the limit of a large  $L_{ICN}$ . We further define the normalized SPR (NSPR) by dividing by the maximum in the parameter range as in

$$NSPR = \frac{SPR}{\max(SP R)}. \quad (2)$$

## IV. Results and Discussion

With the NSPR we derived an expression quantifying the trade-off between power consumption and receive signal strength for combined transmit-receive circuits as shown

in Figure 2. One possible trade-off can be identified at  $-3$  dB that results in halving all harmonics of the receive signal. This point coincides with  $L_{ICN} = L_{DFG}$ , where the inductances match. Consequently, the NSPR indicates that a less attenuated particle signal requires more power (to maintain field specifications). Note, that the same statements are valid if inductances are exchanged, which inverts the ratio  $L_{ICN}/L_{DFG}$ . We simplify the circuit in Figure 2 by considering only the source impedance of the ICN for the inductive voltage divider and not the coupled part from the primary side which creates an offset due to an added series impedance.

Combined TxRx imaging systems on a path towards upscaling for clinical integration face several challenges, including a low-distortion transmit chain and the partial attenuation of the receive signal as stated by (1). In exchange, however, they might have several benefits in comparison to gradiometer topologies. A key requirement for the gradiometer is a sufficiently homogeneous or symmetric excitation field, where two different spatial regions can be separated: A sensitive region where the particles are located (field of view (FOV)) and a region that is insensitive to particles but exposed to the same homogeneous excitation field to be used for cancellation. Especially in the case of saddle coils with a small homogeneous region, a gradiometer becomes very challenging and both suppression and sensitivity are poor. Valuable space in close proximity to the FOV is occupied by dedicated receive coils and thus the transmit chain has to be increased in size, which increases power consumption. A solution might seem to use an entire duplicate system, however, this consumes at least twice the power and provides a lot of possible interference points for distortions, resulting in unequal excitation and cancellation fields for large systems. Consequently, gradiometer topology, coil placement and channel coupling becomes a challenge for large multi-channel systems.

Here, the benefit of a combined TxRx topology might facilitate the process of clinical translation. However, an insight from this study is that a TxRx system with an ICN also requires a twofold power consumption (if  $L_{ICN} = L_{DFG}$ ) and further, that the spectrum of the receive signal is attenuated by the inductive voltage divider. Regarding noise dominance, a reactive voltage divider is lossless and decreases the source impedance without adding thermal noise, which could be combined with a highly parallelized low noise amplifier to compensate the partial signal attenuation.

## Author's statement

Conflict of interest: Authors state no conflict of interest.

## References

- [1] B. Gleich and J. Weizenecker. Tomographic imaging using the nonlinear response of magnetic particles. *Nature*, 435(7046):1214–1217, 2005, doi:[10.1038/nature03808](https://doi.org/10.1038/nature03808).
- [2] B. Gleich, Verfahren zur Ermittlung der räumlichen Verteilung magnetischer Partikel, DE10151778A1, German patent application DE Volume: 101, 2001.
- [3] T. Knopp, N. Gdaniec, and M. Möddel. Magnetic particle imaging: From proof of principle to preclinical applications. *Physics in Medicine & Biology*, 62(14):R124–R178, 2017, Publisher: IOP Publishing. doi:[10.1088/1361-6560/aa6c99](https://doi.org/10.1088/1361-6560/aa6c99).
- [4] J. Weizenecker, B. Gleich, J. Rahmer, H. Dahnke, and J. Borgert. Three-dimensional real-time in vivo magnetic particle imaging. *Physics in Medicine & Biology*, 54(5):L1–L10, 2009, doi:[10.1088/0031-9155/54/5/L01](https://doi.org/10.1088/0031-9155/54/5/L01).
- [5] I. Schmale, B. Gleich, J. Kanzenbach, J. Rahmer, J. Schmidt, J. Weizenecker, and J. Borgert, An introduction to the hardware of magnetic particle imaging, in *IFMBE Proceedings*, ISSN: 1680-0737 Issue: 2, 25, 450–453, Munich, 2009. doi:[10.1007/978-3-642-03879-2\\_127](https://doi.org/10.1007/978-3-642-03879-2_127).
- [6] T. F. Sattel, O. Woywode, J. Weizenecker, J. Rahmer, B. Gleich, and J. Borgert. Setup and validation of an MPI signal chain for a drive field frequency of 150 kHz. *IEEE Transactions on Magnetics*, 51(2):1–3, 2015, Publisher: IEEE.
- [7] B. B. GmbH. Bruker Announces the World's First Preclinical Magnetic Particle Imaging (MPI) System. <https://www.bruker.com/en/products-and-solutions/preclinical-imaging/mpi.html>, 2013. (visited on 02/11/2022).
- [8] M. Graeser, T. Knopp, M. Grüttner, T. F. Sattel, and T. M. Buzug. Analog receive signal processing for magnetic particle imaging. *Medical Physics*, 40(4):42303, 2013, doi:[10.1118/1.4794482](https://doi.org/10.1118/1.4794482).
- [9] H. Paysen, J. Wells, O. Kosch, U. Steinhoff, J. Franke, L. Trahms, T. Schaeffter, and F. Wiekhorst. Improved sensitivity and limit-of-detection using a receive-only coil in magnetic particle imaging. *Physics in Medicine & Biology*, 63(13):13NT02, 2018, doi:[10.1088/1361-6560/aac87](https://doi.org/10.1088/1361-6560/aac87).
- [10] H. Paysen, O. Kosch, J. Wells, N. Loewa, and F. Wiekhorst. Characterization of noise and background signals in a magnetic particle imaging system. *Physics in Medicine & Biology*, 65(23), 2020, Publisher: IOP Publishing. doi:[10.1088/1361-6560/abc364](https://doi.org/10.1088/1361-6560/abc364).
- [11] B. Zheng, W. Yang, T. Massey, P. W. Goodwill, and S. M. Conolly. High-power active interference suppression in magnetic particle imaging, in *2013 International Workshop on Magnetic Particle Imaging, IWMPI 2013*, 1, 2013. doi:[10.1109/IWMPI.2013.6528381](https://doi.org/10.1109/IWMPI.2013.6528381).
- [12] D. Pantke, F. Mueller, S. Reinartz, J. Philipps, S. Mohammadali Dadfar, M. Peters, J. Franke, F. Schrank, F. Kiessling, and V. Schulz. Frequency-selective signal enhancement by a passive dual coil resonator for magnetic particle imaging. *Physics in Medicine & Biology*, 67(11):115004, 2022, doi:[10.1088/1361-6560/ac6a9f](https://doi.org/10.1088/1361-6560/ac6a9f).
- [13] M. Graeser, T. Knopp, P. Szwargulski, T. Friedrich, A. Von Gladiss, M. Kaul, K. M. Krishnan, H. Ittrich, G. Adam, and T. M. Buzug. Towards Picogram Detection of Superparamagnetic Iron-Oxide Particles Using a Gradiometric Receive Coil. *Scientific Reports*, 7(1):6872, 2017, doi:[10.1038/s41598-017-06992-5](https://doi.org/10.1038/s41598-017-06992-5).
- [14] B. Zheng, P. W. Goodwill, N. Dixit, D. Xiao, W. Zhang, B. Gunel, K. Lu, G. C. Scott, and S. M. Conolly. Optimal Broadband Noise Matching to Inductive Sensors: Application to Magnetic Particle Imaging. *IEEE Transactions on Biomedical Circuits and Systems*, 11(5):1041–1052, 2017, doi:[10.1109/TBCAS.2017.2712566](https://doi.org/10.1109/TBCAS.2017.2712566).